PROCEEDINGS OF SCIENCE

Spin in Heavy Ion Collisions : An Experimental Review

Aihong Tang

Brookhaven National Laboratory,
Upton, USA

E-mail: aihong@bnl.gov

The exploration of spin dynamics in heavy ion collisions has become a crucial pathway for unraveling the complex interactions within the fundamental strong force and the angular momentum of subatomic particles. This paper delves into the nuanced aspects of spin physics in the realm of high-energy heavy ion collisions. We investigate the diverse roles that spin plays in revealing the properties of the quark-gluon plasma (QGP), a transient state of matter that existed mere microseconds after the Big Bang. This presentation offers a comprehensive overview of the experimental advancements concerning the global spin effects in heavy ion collisions. Specifically, we address the global polarization of hyperons and the global spin alignment of vector mesons. Furthermore, we explore how these phenomena manifest as outcomes of the intricate dynamics of quarks and gluons within the fireball created in these collisions. This investigation has the potential to offer valuable insights into the properties of strongly interacting QGP matter.

25th International Spin Physics Symposium (SPIN 2023)
24-29 September 2023
Durham, NC, USA

https://pos.sissa.it/

PoS(SPIN2023)230

1. Introduction

In relativistic heavy ion collisions, heavy ions are propelled to velocities nearing the speed of light, leading to dramatic collisions. Within this high-energy interaction, an astounding concentration of energy is deposited within a minuscule volume. This sets the stage for a unique environment where quarks and gluons, usually confined within hadrons, roam freely. It's in this state that they form QGP, a distinct phase of matter believed to have existed existed microseconds after the Big Bang. The laboratory study of these heavy ion collisions [1–4] provides a gateway to profound insights into the evolutionary of the universe.

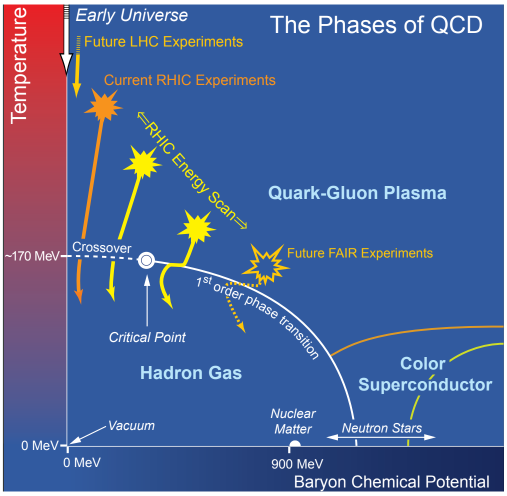

Figure 1: Schematic QCD phase diagram for nuclear matter [5]. The solid lines show the phase boundaries for the indicated phases. The solid circle depicts the critical point.

A primary objective of heavy ion experiments is to unravel the complexities of the Quantum Chromodynamics (QCD) phase diagram, as depicted in Fig. 1. Through the execution of heavy ion collisions at varying energies, we systematically traverse the diverse states of the system at different points on the phase diagram [6]. This process is instrumental in discerning the precise conditions under which ordinary nuclear matter undergoes a transition into QGP. Concurrently, another pivotal mission of heavy ion experiments involves the exploration of the dynamic properties inherent in QCD matter. Thus far, the matter generated has astounded us with its exceptional characteristics: it stands as the hottest known substance [7, 8], exhibiting behavior akin to a nearly perfect liquid with minimal viscosity [1]. Recent findings suggest that this 'liquid' exhibits remarkable vorticity [9] and probably resides within a highly fluctuating strong force field [10].

It is noteworthy that the temporal evolution of heavy ion collisions markedly differs from that of elementary collisions. Heavy ion collisions undergo more prolonged evolution times, characterized by several distinct phases, as illustrated in Fig. 2. These unique steps pave the way for intriguing phenomena exclusive to heavy ion collisions. Recently, we have come to realize that the system possesses a substantial amount of global angular momentum [11], a product of two nuclei hurtling past each other. While some of this angular momentum is carried away by spectator particles, a small fraction is deposited within the interaction regions, giving rise to vorticity fields. See Fig. 3 for a typical setup of relativistic heavy ion collisions. These locally swirling vorticity fields interact

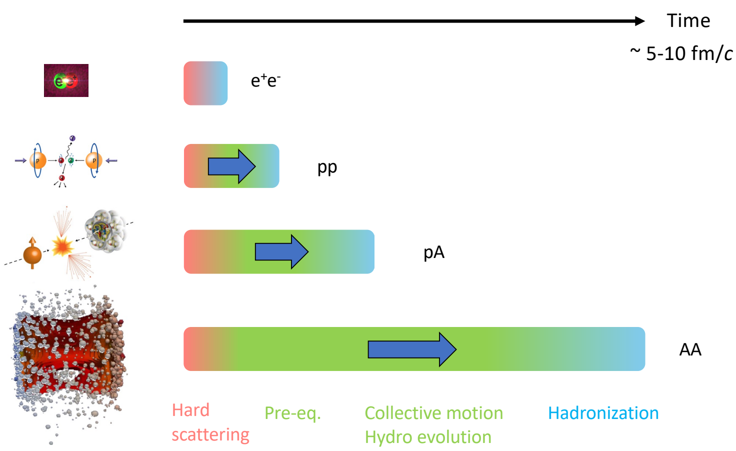

Figure 2: Temporal evolution of heavy ion collisions.

with particles through spin-orbital coupling, influencing their spin properties. Thus, stemming from the initial global angular momentum, the system becomes globally polarized(see reviews [12, 13] and references therein)—a distinctive feature in heavy ion collisions. In essence, particles within the system exhibit collective polarization.

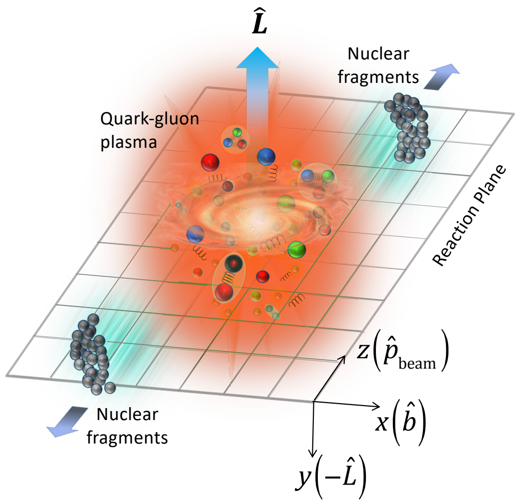

Figure 3: Schematic view of relativistic heavy ion collisions. The two nuclei passing by create a rotation in the middle, give rise vorticity fields. $\hat{L}$ denotes the global angular momentum.

2. Hyperon global polarization

The global polarization mentioned above is at quark level, but can be effectively studied through the polarization in hyperons such as Λ's. Λ is the lightest hyperon containing a strange quark, with the polarization of the Λ hyperon solely attribute to the polarization of strange quark. The decay of $\Lambda \to \pi^- + p$ involves a parity-violating weak decay, and the proton tends to go off in the direction of Λ's spin. In practice, the Λ polarization parameter, denoted as P_H, is determined by fitting the distribution of the angle (θ^*)—measured in the Λ's rest frame—between the proton momentum and the polarization axis. The distribution is described as $\frac{dN}{d\Omega^*} = \frac{1}{4\pi}(1 + \alpha_{\mathrm{H}}\mathrm{P}_{\mathrm{H}}\cos\theta^*)$, where α_{H} is the decay parameter for Λ, and P_H signifies the polarization of Λ.

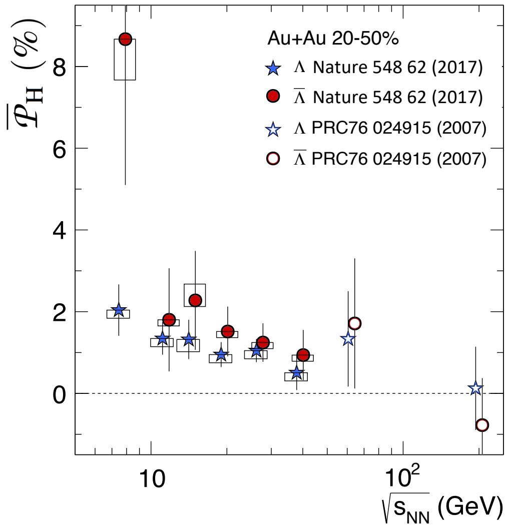

Figure 4: Global polarization of $\Lambda(\bar{\Lambda})$ hyperon as a function of collision energy.

The STAR experiment at RHIC has reported noteworthy findings on the global polarization of Λ hyperons in relation to collision energy [9]. This polarization exhibits a discernible value at lower energies and displays a gradual decline with increasing energy (see Fig. 4). Initially, this trend was attributed to the presence of thermal vorticity [14]. At higher energies, the fireball at middle rapidities maintain characteristics akin to a boost-invariant fluid, resulting in diminished vorticity and, consequently, a decrease in the observed P_{H}. However, as more data emerged, discrepancies in the measurements of global polarization, particularly with respect to the azimuthal angle relative to the reaction plane, became apparent. The data indicated that P_{H} exhibited its strongest manifestation in the in-plane direction, diminishing out-of-plane (depicted as P^{J} in Fig. 5(a)). Another discrepancy is seen in the measurement of polarization along the beam direction (z-axis) concerning azimuthal angle (P^{z} in Fig. 5(c)). These measurements revealed intricate substructures within the vorticity field. Specifically, the global vorticity field appeared strongest in-plane, and the local vorticity field along the beam direction aligned with a robust elliptic flow expansion along the in-plane direction. The prevailing framework at that time, primarily considering the thermal vorticity, failed to predict the observed trends for both sets of measurements, resulting in what became known as the "sign puzzle". This puzzling discrepancy prompted the scientific community to explore additional mechanisms that might have been overlooked. More recently, it has been realized that incorporating other contributions, particularly those arising from thermal shear, could provide a resolution to the sign puzzle. The inclusion of thermal shear, characterized by the antisymmetric gradient of the four-temperature, yielded predictions (see Fig. 5(b) and Fig. 5(d)) that align better with the observed trends in the data.

Nonetheless, the observed concordance hinges on a delicate equilibrium between thermal vorticity and thermal shear, both wielding considerable influence but acting in opposing directions. Even a slight modification in either of these factors could exert a significant impact on the out-

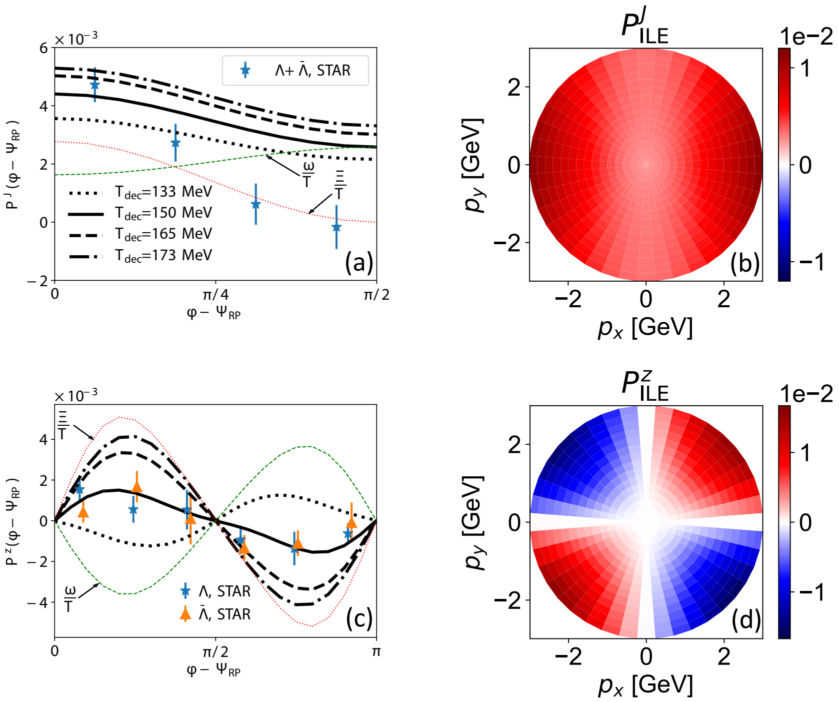

Figure 5: Left column : The global polarization [15] (a) and local polarization in beam direction [16] (b) as a function of azimuthal angle. The contribution from thermal vorticity ($\frac{\omega}{T}$) and thermal shear ($\frac{\Xi}{T}$) are indicated as green and red dotted lines, respectively. Right column : the theoretical calculations [17] of the corresponding polarization as a function of its transverse momentum (p_x, p_y), with the contribution from thermal shear included.

comes. Throughout this investigation, we also discerned the susceptibility of the results to several other variables. For example, in the theoretical calculations portrayed in Fig.5, variations in the deconfinement temperature produced substantial alterations in the results. Moreover, grappling with nuances such as why T-vorticity adheres to the correct trend[18] and comprehending the significance of scenarios like the s-quark memory, which elucidates the observed data trend [19], presents an ongoing challenge. Gaining proficiency in managing these variables to ensure stability and reliability in our predictions remains an active pursuit within the scientific community.

The utilization of collective polarization patterns stands as a valuable methodology for investigating the characteristics of hot dense matter formed during relativistic heavy ion collisions. By altering the system size, one can scrutinize how the global polarization reacts to variations in the vorticity profile across different systems. The anticipation is that larger systems uphold superior boost invariance at middle rapidities, resulting in diminished vorticity and, consequently, a reduction in global polarization [22, 23]. The STAR experiment delved into the examination of global polarization in Λ particles arising from $^{96}_{44}$Ru $+^{96}_{44}$ Ru and $^{96}_{40}$Zr $+^{96}_{40}$ Zr collisions [20], comparing the outcomes with those from $^{197}_{79}$Au $+^{197}_{79}$ Au collisions (Fig. 6(a)). Surprisingly, despite a nearly twofold difference in the number of nucleons between $^{197}_{79}$Au and $^{96}_{44}$Ru (or $^{96}_{40}$Zr) ions, no significant distinctions were discerned within the margin of error. While acknowledging the noteworthy uncertainty inherent in the measurements, this observation prompts further reflection and analysis.

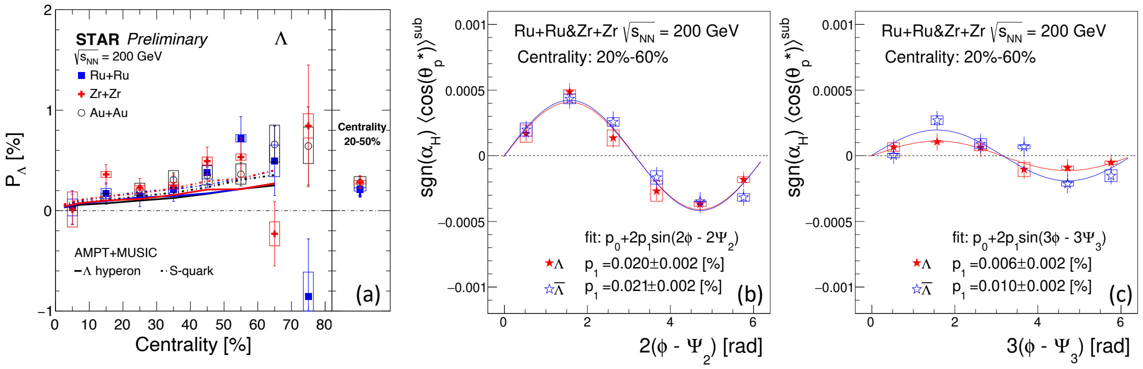

Figure 6: (a) Global polarization of Λ hyperon as a function of centrality in ${}^{197}_{79}$Au $+{}^{197}_{79}$ Au, ${}^{96}_{44}$Ru $+{}^{96}_{44}$ Ru and ${}^{96}_{40}$Zr $+{}^{96}_{40}$ Zr collisions at $\sqrt{s_{NN}}$ = 200 GeV [20]. (b) and (c) : Λ and $\bar{\Lambda}$ polarization along the beam-axis as a function of azimuthal angle with respect to second (b) and third (c) order event plane [21].

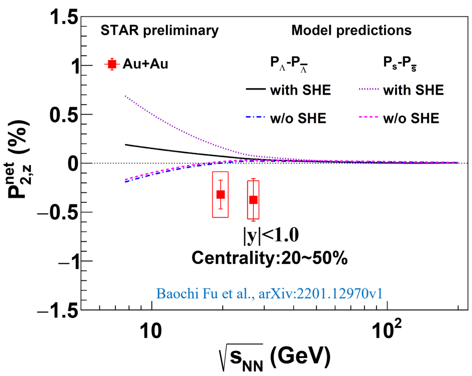

Figure 7: Baryonic Spin Hall Effect, as quantified by $P_\Lambda - P_{\bar{\Lambda}}$, as a function of collision energy.

The spin phenomena also give rise to other intriguing effects. One such phenomenon is the Spin Hall effect, which involves the generation of spin current in materials when spin carriers are in motion under an external electric field. This effect has been observed in semiconductors, metals, and insulators at or below room temperature. Recent theoretical developments [24–26] indicate that the spin Hall current can be induced by the gradient of the baryon chemical potential, serving as an analogous electric field. This effect leads to the polarization separation between Λ and $\bar{\Lambda}$, with a more pronounced impact at lower energies. Ongoing experimental efforts are dedicated to studying this phenomenon, and Fig. 7 presents STAR's preliminary results [27] on the baryonic spin Hall effect. The current uncertainty associated with the data points prevents us from drawing firm conclusions; however, there is optimism that with increased statistical data at lower energy levels, where the effect is more prominent, we may observe and understand this effect more comprehensively.

3. Vector meson global spin alignment

The exploration of collective spin phenomena extends to the realm of vector mesons. In the case of spin-1 vector mesons like ϕ and K^{*0}, their spin states are described by a 3×3 spin density matrix. The diagonal element ρ_{00} specifically denotes the likelihood of finding a vector meson in spin state 0 within the three possible spin states (-1, 0, and 1). In the absence of spin alignment, ρ_{00} stands at 1/3; however, when there is spin alignment, ρ_{00} deviates from this baseline. The process of determining ρ_{00} from data mirrors the hyperon spin polarization analysis, with the distinction that the angle distribution of a daughter and the quantization axis in the meson's rest frame is fitted with an even function instead of an odd one: $\frac{dN}{d(\cos\theta^*)} \propto (1-\rho_{00}) + (3\rho_{00}-1)\cos^2\theta^*$.

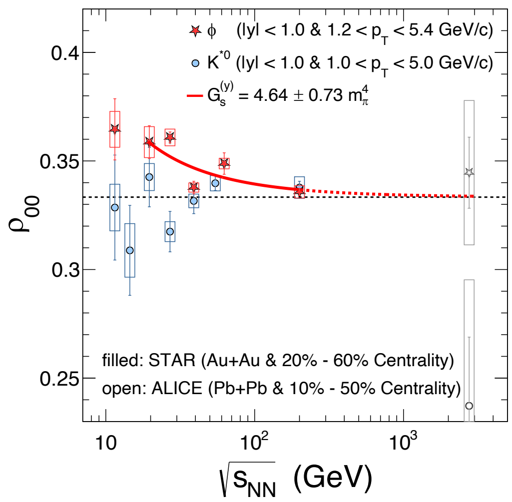

Figure 8: Global spin alignment of ϕ and K^{*0} as a function of collision energy [10]. The red solid curve represents the fit to ϕ data using a model based on ϕ-meson strong force field.

The STAR experiment recently presented findings on the ρ_{00} measurements for ϕ and K^{*0} across varying collision energies [10]. Intriguingly, the ϕ-meson displayed substantial global spin alignment, while the K^{*0}-meson exhibited minimal alignment (see Fig. 8). This observation introduces intricacies, considering that the presumed sources contributing to the global spin alignment of ϕ-mesons—including quark coalescence with vorticity and magnetic field, the electric component of the vorticity tensor, classic electric field contributions, and fragmentation—are conventionally at the 10^{-4} or 10^{-5} level, proving inadequate to account for the observed data. The introduction of additional factors, such as local spin alignment and turbulent color fields, negatively influences ρ_{00}, suggesting the involvement of novel mechanisms contributing to the significant ρ_{00} in ϕ-mesons.

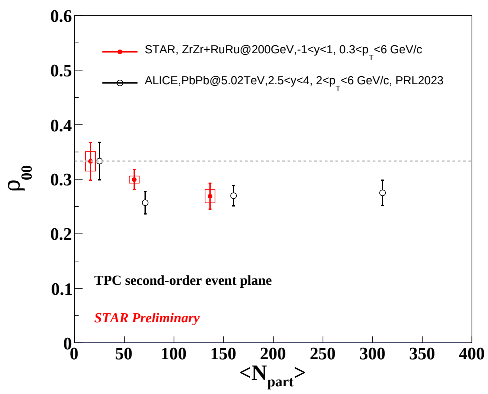

Figure 9: ρ_{00} of J/ψ as a function of number of participants, measured by STAR [31] and ALICE [30].

Two recent proposed models delve into the local fluctuation of the strong force field of vector mesons [28] and fluctuations of the glasma fields [29]. These models potentially offer explanations for the observed substantial signal. Notably, the contribution from the strong force field of vector mesons appears capable of explaining both the magnitude and, to some extent, the energy dependence (refer to ref. [28] and related references). This observation underscores the pivotal role of the strong force field in influencing quark spin, emphasizing that ρ_{00} is sensitive to local field fluctuations—an aspect in stark contrast to hyperon polarization, which predominantly responds to its mean value.

One specific rationale enabling the theoretical calculation of ρ_{00} for ϕ-mesons lies in the fact that the two quarks composing the ϕ-meson belong to the same flavor family, making the calculation easy to perform. This characteristic also renders the ρ_{00} measurement for J/ψ intriguing, given that it comprises c and $\bar{c}$ quarks, both come from the same flavor family. Both ALICE [30] and STAR [31] have conducted this measurement. Fig. 9 displays ρ_{00} of J/ψ measured as a function of number of participants. The number of participants denotes the count of actively involved nucleons from colliding heavy ions. The largest number corresponds to the collision with the most overlap region of two nuclei. It seems that except for very peripheral collisions (low minimal participants), the ρ_{00} of J/ψ are smaller than 1/3 . In addition, they exhibits the same value at the same at same $\langle N_{part} \rangle$. The naive expectation from fluctuating strong force field would be that ρ_{00} of J/ψ is greater than 1/3, at least at middle rapidity. The observation does not seem to fit in the picture, however, when considering $J\psi$, one has to take into account other complexity like color screening effect etc. A more comprehensive understanding and control of different contributions are needed in order to understand the result.

In Fig. 10, the ρ_{00} is depicted as a function of transverse momentum, compared with the newly measured prompt D^+ meson. Notably, the J/ψ exhibits a ρ_{00} that is below 1/3 at low p_T, whereas the D^+ meson showcases a value exceeding 1/3, both seemingly escalating with increasing p_T. The interpretation of these results necessitates additional theoretical insights for a comprehensive understanding.

STAR [33] and ALICE [32] presented findings on the rapidity dependence of ρ_{00} for ϕ and D^{*+}-mesons, respectively (Fig. 11). Both observations highlight a significant rise in ρ_{00} with increasing rapidity. The STAR results are compared with theoretical predictions grounded in the strong force field, revealing a consistent trend. According to this particular theory, the observed pattern stems from the increased prominence of fluctuations in the direction perpendicular to the motion.

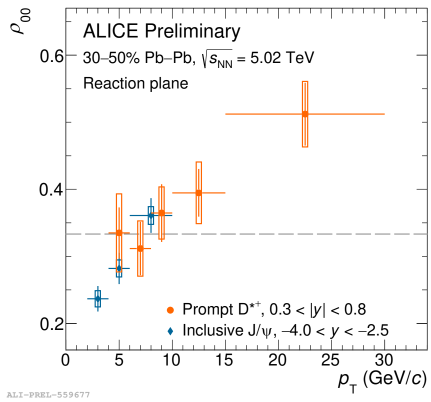

Figure 10: ρ_{00} measured as a function of transverse momentum for J/ψ and D^{*+} [32].

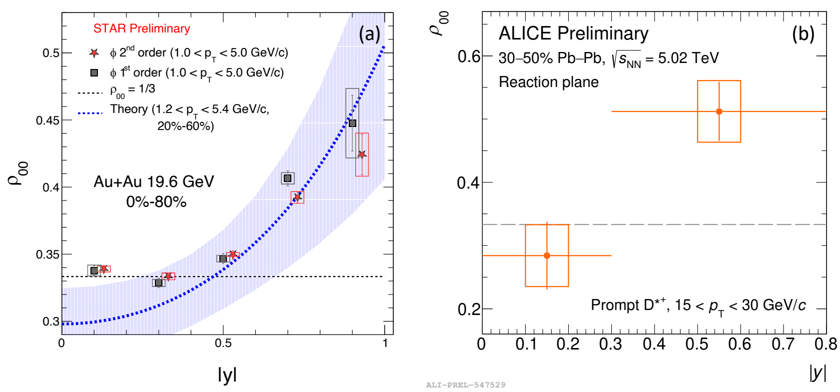

Figure 11: Rapidity dependenc of ρ_{00} measured by STAR [33] and ALICE [32].

4. Conclusion

In this paper, we have provided a comprehensive overview of the experimental advancements in understanding spin phenomena within relativistic heavy ion collisions. The unique character of heavy ion collisions unveils an intriguing interplay of fundamental forces, giving rise to a system-wide, global spin polarization—a characteristic absent in elementary collisions. The exploration of hyperon polarization, with its initially puzzling sign dilemma and subsequent resolution, has cast light on the intricate vortical structures within the quark-gluon plasma. The unexpected prominence of ρ_{00} in ϕ-mesons, challenging conventional theoretical frameworks, along with its dependence on rapidity, deepens our insight into the influential role played by the strong force under extreme conditions. Extending our investigations to include J/ψ and D^+ mesons promises additional perspectives on this intriguing realm.

The study of spin in heavy ion collisions is a thriving and promising field that delves into the fascinating behavior of particles' global spin features under extreme conditions. Despite its relatively short history, this field has already yielded remarkable discoveries, such as the observation of the most vortical fluid known and tantalizing hints of a strongly fluctuating strong force field. As is typical in newly established domains, numerous unanswered questions beckon, presenting fertile ground for future exploration and research endeavors.

References

[1] STAR collaboration, *Experimental and theoretical challenges in the search for the quark gluon plasma: The STAR Collaboration's critical assessment of the evidence from RHIC collisions*, Nucl. Phys. A **757** (2005) 102 [nucl-ex/0501009].

[2] PHENIX collaboration, *Formation of dense partonic matter in relativistic nucleus-nucleus collisions at RHIC: Experimental evaluation by the PHENIX collaboration*, Nucl. Phys. A **757** (2005) 184 [nucl-ex/0410003].

[3] PHOBOS collaboration, *The PHOBOS perspective on discoveries at RHIC*, Nucl. Phys. A **757** (2005) 28 [nucl-ex/0410022].

[4] BRAHMS collaboration, *Quark gluon plasma and color glass condensate at RHIC? The Perspective from the BRAHMS experiment*, Nucl. Phys. A **757** (2005) 1 [nucl-ex/0410020].

[5] T.D.N.S.A. Committee, *The frontiers of nuclear science, a long range plan*, 2008.

[6] STAR collaboration, *Bulk Properties of the Medium Produced in Relativistic Heavy-Ion Collisions from the Beam Energy Scan Program*, Phys. Rev. C **96** (2017) 044904 [1701.07065].

[7] PHENIX collaboration, *Enhanced production of direct photons in Au+Au collisions at $\sqrt{s_{NN}} = 200$ GeV and implications for the initial temperature*, Phys. Rev. Lett. **104** (2010) 132301 [0804.4168].

[8] ALICE collaboration, *Measurement of Direct Photons in pp and Pb-Pb Collisions with ALICE*, Nucl. Phys. A **904-905** (2013) 573c [1210.5958].

[9] STAR collaboration, *Global Λ hyperon polarization in nuclear collisions: evidence for the most vortical fluid*, Nature **548** (2017) 62 [1701.06657].

[10] STAR collaboration, *Pattern of global spin alignment of ϕ and K^{*0} mesons in heavy-ion collisions*, Nature **614** (2023) 244 [2204.02302].

[11] Z.-T. Liang and X.-N. Wang, *Globally polarized quark-gluon plasma in non-central A+A collisions*, *Phys. Rev. Lett.* **94** (2005) 102301 [nucl-th/0410079].

[12] F. Becattini, J. Liao and M. Lisa, *Strongly Interacting Matter Under Rotation: An Introduction*, *Lect. Notes Phys.* **987** (2021) 1 [2102.00933].

[13] F. Becattini, *Spin and polarization: a new direction in relativistic heavy ion physics*, *Rept. Prog. Phys.* **85** (2022) 122301 [2204.01144].

[14] F. Becattini, I. Karpenko, M. Lisa, I. Upsal and S. Voloshin, *Global hyperon polarization at local thermodynamic equilibrium with vorticity, magnetic field and feed-down*, *Phys. Rev. C* **95** (2017) 054902 [1610.02506].

[15] STAR collaboration, *Global and local polarization of Λ hyperons in Au+Au collisions at 200 GeV from STAR*, *Nucl. Phys. A* **982** (2019) 511 [1808.10482].

[16] STAR collaboration, *Polarization of Λ ($\bar{\Lambda}$) hyperons along the beam direction in Au+Au collisions at $\sqrt{s_{NN}}$ = 200 GeV*, *Phys. Rev. Lett.* **123** (2019) 132301 [1905.11917].

[17] F. Becattini, M. Buzzegoli, G. Inghirami, I. Karpenko and A. Palermo, *Local Polarization and Isothermal Local Equilibrium in Relativistic Heavy Ion Collisions*, *Phys. Rev. Lett.* **127** (2021) 272302 [2103.14621].

[18] H.-Z. Wu, L.-G. Pang, X.-G. Huang and Q. Wang, *Local spin polarization in high energy heavy ion collisions*, *Phys. Rev. Research.* **1** (2019) 033058 [1906.09385].

[19] B. Fu, S.Y.F. Liu, L. Pang, H. Song and Y. Yin, *Shear-Induced Spin Polarization in Heavy-Ion Collisions*, *Phys. Rev. Lett.* **127** (2021) 142301 [2103.10403].

[20] X. Gou for STAR, Quark Matter 2023.

[21] STAR collaboration, *Hyperon polarization along the beam direction relative to the second and third harmonic event planes in isobar collisions at $\sqrt{s_{NN}}$ = 200 GeV*, 2303.09074.

[22] S. Alzhrani, S. Ryu and C. Shen, *Λ spin polarization in event-by-event relativistic heavy-ion collisions*, *Phys. Rev. C* **106** (2022) 014905 [2203.15718].

[23] S. Shi, K. Li and J. Liao, *Searching for the Subatomic Swirls in the CuCu and CuAu Collisions*, *Phys. Lett. B* **788** (2019) 409 [1712.00878].

[24] S.Y.F. Liu and Y. Yin, *Spin Hall effect in heavy-ion collisions*, *Phys. Rev. D* **104** (2021) 054043 [2006.12421].

[25] X.-Y. Wu, C. Yi, G.-Y. Qin and S. Pu, *Local and global polarization of Λ hyperons across RHIC-BES energies: The roles of spin hall effect, initial condition, and baryon diffusion*, *Phys. Rev. C* **105** (2022) 064909 [2204.02218].

[26] B. Fu, L. Pang, H. Song and Y. Yin, *Signatures of the spin Hall effect in hot and dense QCD matter*, 2201.12970.

[27] Q. Hu for STAR, Workshop on Chirality, Vorticity and Magnetic Field in Heavy Ion Collisions, 2023.

[28] X.-L. Sheng, L. Oliva, Z.-T. Liang, Q. Wang and X.-N. Wang, *Spin Alignment of Vector Mesons in Heavy-Ion Collisions*, *Phys. Rev. Lett.* **131** (2023) 042304 [2205.15689].

[29] A. Kumar, B. Müller and D.-L. Yang, *Spin alignment of vector mesons by glasma fields*, *Phys. Rev. D* **108** (2023) 016020 [2304.04181].

[30] ALICE collaboration, *Measurement of the J/ψ Polarization with Respect to the Event Plane in Pb-Pb Collisions at the LHC*, *Phys. Rev. Lett.* **131** (2023) 042303 [2204.10171].

[31] D. Shen for STAR, Spin2023; B. Xi for STAR, QM2023.

[32] L. Micheletti for ALICE, Quark Matter 2023.

[33] G. Wilks for STAR, Spin 2023.

PoS(SPIN2023)230